VOLUME 113, NUMBER 11
MAY 22, 1991

JOURNAL
OF THE
AMERICAN
CHEMICAL
SOCIETY

Variable-Temperature Variable-Field Magnetic Circular Dichroism Studies of the Fe(II) Active Site in Metapyrocatechase: Implications for the Molecular Mechanism of Extradiol Dioxygenases

Patricia A. Mabrouk,[†] Allen M. Orville,[‡] John D. Lipscomb,[‡] and Edward I. Solomon*,[†]

Contribution from the Department of Chemistry, Stanford University, Stanford, California 94305, and Department of Biochemistry, University of Minnesota, Minneapolis, Minnesota 55455.
Received August 20, 1990

Abstract: A combination of optical absorption, circular dichroism (CD), and magnetic circular dichroism (MCD) spectroscopies has been used to probe the geometric and electronic structure of the catalytically relevant Fe^{2+} active site in metapyrocatechase (catechol 2,3-dioxygenase). The number and energies of the excited-state ligand field features have been used to define the effective active site geometry. The magnetic field and temperature dependence of the MCD intensity of the excited-state ligand field features have been used to determine the ground-state zero-field splitting and g values for the EPR inactive $S = 2$ center. Ligand field diagrams have been constructed on the basis of experimental estimates of the e and t_2 d orbital splittings derived from the excited-state and ground-state analyses, respectively. A 5-coordinate square-pyramidal effective geometry is obtained for the active site of resting metapyrocatechase. Spectroscopic evidence is presented for the binding of substrate (catechol) to the active site Fe^{2+}. Catechol appears to bind in a bidentate fashion, occupying the axial site and one equatorial position at the ferrous center. Addition of azide to the enzyme causes no change in the MCD spectrum, suggesting that azide does not bind to the iron. However, substrate binding to the iron activates the enzyme toward azide binding. A square-pyramidal geometry is also found for this ternary complex, with azide occupying an equatorial ligation site at the ferrous center. Geometric and electronic structural changes resulting from the addition of substrate and azide to resting metapyrocatechase are discussed in terms of their relevance to the catalytic mechanism for the extradiol dioxygenases.

Introduction

The active sites of a number of non-heme metalloproteins contain a mononuclear high-spin Fe^{2+} center that has been implicated in the binding and catalytic activation of molecular oxygen.[1] Limited progress has been made in the study of the structure and mechanism of these metalloenzymes due to the spectroscopic inaccessibility of the Fe^{2+} center. High-spin Fe^{2+} does not exhibit low-energy ligand to metal charge-transfer transitions. Study of the weak ($\epsilon < 10\ M^{-1}\ cm^{-1}$) ligand field features is prohibited by the relatively low concentrations, typically less than millimolar, possible for large molecular weight proteins. Furthermore, Fe^{2+} is a non-Kramers $S = 2$ system and is often EPR silent due to zero-field splitting and fast relaxation effects. Application of Mössbauer spectroscopy to these systems has been limited; even when ^{57}Fe incorporation is possible, resolvable magnetic field effects have not been reported. Finally, crystallographic information on non-heme Fe^{2+} enzymes is not currently available.[2]

[†] Stanford University.
[‡] University of Minnesota.

(1) (a) Phenylalanine hydroxylase: Dix, T. A.; Benkovic, S. J. *Acc. Chem. Res.* **1988**, *21*, 101. (b) Bleomycin: Hecht, S. M. *Acc. Chem. Res.* **1986**, *19*, 383. (c) Soybean lipoxygenase: Veldink, G. A.; Vliegenthart, J. F. G. *Adv. Inorg. Biochem.* **1984**, *6*, 139. (d) Superoxide dismutase: Slykhouse, T. O.; Fee, J. A. *J. Biol. Chem.* **1976**, *251*, 5472. (e) Thymine hydroxylase: Warn-Cramer, B. J.; Macrander, L. A.; Abbott, M. T. *J. Biol. Chem.* **1983**, *258*, 10551. (f) ω-Hydroxylase: Ruettinger, R. T.; Griffith, G. R.; Coon, M. J. *Arch. Biochem. Biophys.* **1977**, *183*, 528. (g) Gentisate 1,2-dioxygenase: Harpel, M. R.; Lipscomb, J. D. *J. Biol. Chem.* **1990**, *265*, 6301.

0002-7863/91/1513-4053$02.50/0

One important class of non-heme Fe^{2+} enzymes is the extradiol dioxygenases.[3] These metalloproteins catalyze the extradiol ring cleavage of catechol or its derivatives with the insertion of both atoms of molecular oxygen. Extradiol dioxygenases include such enzymes as protocatechuate 4,5-dioxygenase[4] from *Pseudomonas testosteroni*, 3,4-dihydroxyphenylacetate 2,3-dioxygenase[5] from *Pseudomonas ovalis*, and metapyrocatechase[6] from *Pseudomonas putida*. Metapyrocatechase, which contains 4 mol of Fe^{2+}/molecule (MW = 140 000) and has four identical subunits per molecule, catalyzes the extradiol ring cleavage of catechol with the insertion of molecular oxygen to produce α-hydroxymuconic ϵ-semialdehyde.

Progress in the study of metapyrocatechase has been limited by both the aforementioned spectroscopic inaccessibility of Fe^{2+} as well as protein instability (metapyrocatechase is slowly inactivated in air). Mössbauer spectroscopy of ^{57}Fe-reconstituted metapyrocatechase and the anaerobic enzyme–substrate complex has confirmed the presence of high-spin Fe^{2+} in the active site (δ = 1.31 mm/s; ΔE_Q = 3.28 mm/s) and suggested that substrate binding does not change the coordination environment of the Fe^{2+} site.[7] Recently, EPR studies on an NO complex of metapyrocatechase, which exhibits an $S = {}^3/_2$ EPR signal, have provided evidence for the presence of several sites at the iron center that are available for exogenous ligand binding.[4b,4c] Nonetheless, the metapyrocatechase Fe^{2+} active site coordination geometry, the nature of the ligands, and the steps of the catalytic mechanism remain unknown.

We have recently developed a spectroscopic protocol for the study of Fe^{2+} active sites in non-heme metalloenzymes that is based on the combined use of optical absorption (ABS), circular dichroism (CD), and variable-temperature variable-field magnetic circular dichroism (MCD) spectroscopies.[8] The approach is 2-fold: Optical absorption, CD, and MCD spectroscopies, each of which has different selection rules, are used to obtain the Fe^{2+} ligand field excited-state features of the enzyme active site that appear in the near-IR spectral region. The number and energies of the d → d excited states can be used to define an effective geometry at the Fe^{2+} center on the basis of ligand field effects. A 6-coordinate ferrous ion has a pair of spin-allowed ligand field transitions at about 10 000 cm^{-1} split by <2000 cm^{-1}. Five-coordinate iron, on the other hand, is associated with the presence of one ligand field band near 10 000 cm^{-1} and a second band near 5000 cm^{-1}, while ferrous ion in a tetrahedral coordination environment only exhibits a set of transitions in the 5000 cm^{-1} region.

Complementary information on orbital splitting of the $^5T_{2g}$ ground state is obtained through the quantitative analysis of the field and temperature dependence of the MCD intensity for the ferrous excited-state ligand field spectral features. The magnetization saturation behavior observed for an $S = 2$ ground state with a negative axial zero-field splitting parameter (D) has been quantitatively explained by Zeeman mixing within an isolated rhombically split non-Kramers $M_s = \pm 2$ doublet. The magnitude of this rhombic splitting (δ) has in turn been related to the magnitude of the axial (Δ ($\equiv E_{xy} - E_{xz,yz}$)) and rhombic ($V$ ($\equiv E_{xz} - E_{yz}$)) orbital splitting within the Fe^{2+} $^5T_{2g}$ ground state and to the Fe^{2+} active site geometry.

The specific aim of the present study has been the application of this protocol to determine the geometric and electronic structure of the active site of metapyrocatechase and to probe substrate and small molecule complexes related to metapyrocatechase's catalytic mechanism. We have now completed detailed ABS, CD, and variable-temperature variable-field MCD studies of resting, anaerobic substrate and substrate-activated azide-bound forms of metapyrocatechase. We have found variable-temperature variable-field MCD to be a very sensitive probe of active site geometry, electronic structure, and structural changes associated with substrate and ligand binding at the ferrous site. These studies have provided significant insight into the active site in metapyrocatechase and establish the utility of this spectroscopic protocol in obtaining molecular level insight into catalytic processes in non-heme Fe^{2+} enzymes.

Experimental Section

Metapyrocatechase was isolated from *P. putida* (ATCC 23973) maintained on *meta*-toluic acid, grown on benzoate as the sole carbon source, and purified according to a procedure previously described.[4b] The specific activity was typically >300 units/mg. The Fe^{2+} concentration was typically 4–8 mM. The buffer used in all cases was 50 mM potassium phosphate (pH 7.5) plus 10% (v) acetone to protect the enzyme from inactivation in air.

The following materials were purchased and used as obtained: D_2O (99.9 atom % D; Aldrich), NaOD (40 wt % in D_2O; Aldrich), DCl (37 wt % in D_2O; Aldrich), acetone-d_6 (Aldrich), phosphoric acid-d_3 (85 wt % in D_2O; Aldrich), glycerol (Baker), sodium hydrosulfite (Fisher), and sodium azide (Aldrich). Catechol (Sigma) was sublimed in vacuo and stored under dry N_2 in the dark.

Near-IR optical absorption spectra (800–1100 nm) at 298 K were obtained on a Cary 17 UV/vis spectrophotometer. UV/vis absorption spectra (190–820 nm) at 298 K were recorded on an HP 8452A diode array spectrometer. Low-temperature (1.6–65 K) CD and MCD spectra (450–1100 nm) were recorded on a Jasco J500C spectropolarimeter equipped with an Oxford SM4-6T magnet. MCD spectra were recorded at applied magnetic fields up to 5.9 T. Room temperature near-IR CD spectra (650–2000 nm) were obtained on a Jasco J200 spectropolarimeter with use of a 1 mm path length cell.

The low-temperature MCD cell consisted of two quartz disks (12-mm diameter) sandwiching a 3-mm-thick rubber o-ring spacer (5-mm i.d.; 1.2-mm o.d.). The effective sample volume of the MCD cell is 60 μL. Ferrous concentrations of greater than 1 mM are desirable.

In order to measure the NIR-ABS and CD spectra (1800–2150 nm) of metapyrocatechase, H_2O in the protein sample was exchanged with D_2O by repeated (5×) dilution with 50 mM D_3PO_4/D_2O (pD 7.55) plus 10% (v) acetone-d_6 and subsequent concentration in an Amicon ultrafiltration cell (Amicon Corp., MA) with use of a YM 30 Diaflo Ultrafillter (Millipore Corp., MA) or with use of a Millipore CX-30 immersible ultrafiltration cell.

All protein samples used in low-temperature CD/MCD (<65 K) were studied as glasses in degassed 50% (v/v) glycerol/50 mM potassium phosphate buffer plus 10% (v) acetone. Enzyme samples were made anaerobic as described in an earlier paper.[4c] Microliter quantities of dithionite were added to ensure the absence of oxygen. Addition of sodium dithionite was found to produce no change in the appearance of either the CD or MCD spectrum.

Depolarization of the protein glasses studied was checked by measuring the CD of a freshly prepared nickel tartrate solution placed immediately before and after the sample in the spectrometer.[9] All samples

(2) Recently two reports have appeared detailing the crystallization and preliminary X-ray characterization of two isozymes of soybean lipoxygenase: (a) Steczko, J.; Smith, J. L.; Axelrod, B. *J. Biol. Chem.* **1990**, *265*, 11352. (b) Stallings, W. C.; Kroa, B. A.; Carroll, R. T.; Metzger, A. L.; Funk, M. O. *J. Mol. Biol.* **1990**, *211*, 685.

(3) (a) Nozaki, M. *Top. Curr. Chem.* **1979**, *78*, 145. (b) Lipscomb, J. D.; Whittaker, J. W.; Arciero, D. M. In *Oxygenases and Oxygen Metabolism—4 Symposium in Honor of Osamu Hayaishi*; Nozaki, M., Yamamoto, S., Coon, M. J., Ernster, L., Estabrook, R. W., Eds.; Academic Press: New York, 1982; pp 27–37.

(4) (a) Arciero, D. M.; Lipscomb, J. D.; Huynh, B. H.; Kent, T. A.; Münck, E. *J. Biol. Chem.* **1983**, *258*, 14981. (b) Arciero, D. M.; Orville, A. M.; Lipscomb, J. D. *J. Biol. Chem.* **1985**, *260*, 14035. (c) Arciero, D. M.; Lipscomb, J. D. *J. Biol. Chem.* **1986**, *261*, 2170.

(5) (a) Kita, H. *J. Biochem. (Tokyo)* **1965**, *58*, 116. (b) Kita, H.; Miyake, Y.; Kamimoto, M.; Senoh, S. *J. Biochem. (Tokyo)* **1969**, *66*, 45. (c) Ono-Kamimoto, M. *J. Biochem. (Tokyo)* **1973**, *74*, 1049. (d) Ono-Kamimoto, M.; Senoh, S. *J. Biochem. (Tokyo)* **1974**, *75*, 321.

(6) (a) Kojima, Y.; Itada, N.; Hayaishi, O. *J. Biol. Chem.* **1961**, *236*, 2223. (b) Nozaki, M.; Kagamiyama, H.; Hayaishi, O. *Biochem. Biophys. Res. Commun.* **1963**, *11*, 65. (c) Nozaki, M.; Kagamiyama, H.; Hayaishi, O. *Biochem. Z.* **1963**, *338*, 582. (d) Nozaki, M.; Ono, K.; Nakazawa, T.; Kotani, S.; Hayaishi, O. *J. Biol. Chem.* **1968**, *243*, 2682. (e) Nozaki, M.; Kotani, S.; Ono, K.; Senoh, S. *Biochim. Biophys. Acta* **1970**, *220*, 213. (f) Hirata, F.; Nakazawa, A.; Nozaki, M.; Hayaishi, O. *J. Biol. Chem.* **1971**, *246*, 5882. (g) Hori, K.; Hashimoto, T.; Nozaki, M. *J. Biochem. (Tokyo)* **1973**, *74*, 375. (h) Sternson, L. A.; Sternson, A. E. *Chem.-Biol. Interact* **1973**, *7*, 143. (i) Nakai, C.; Hori, K.; Kagamiyama, H.; Nakazawa, T.; Nozaki, M. *J. Biol. Chem.* **1983**, *258*, 2916. (j) Nakai, C.; Kagamiyama, H.; Nozaki, M.; Nakazawa, T.; Inouye, S.; Ebina, Y.; Nakazawa, A. *J. Biol. Chem.* **1983**, *258*, 2923. (k) Nozaki, M. *Methods Enzymol.* **1970**, *17A*, 522–525.

(7) Tatsuno, Y.; Saeki, Y.; Nozaki, M.; Otsuka, S.; Maeda, Y. *FEBS Lett.* **1983**, *112*, 83.

(8) (a) Whittaker, J. W.; Solomon, E. I. *J. Am. Chem. Soc.* **1986**, *108*, 835. (b) Whittaker, J. W.; Solomon, E. I. *J. Am. Chem. Soc.* **1988**, *110*, 5329.

(9) Browett, W. R.; Fucaloro, A. F.; Morgan, T. V.; Stephens, P. J. *J. Am. Chem. Soc.* **1983**, *105*, 1868.

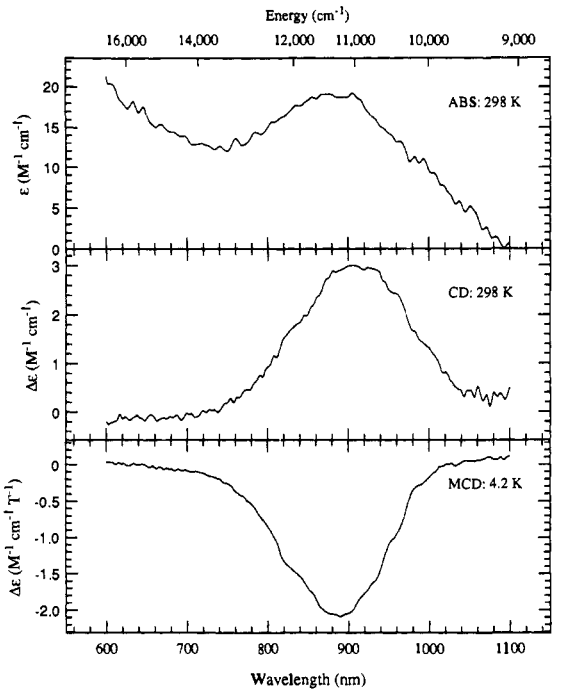

Figure 1. Ligand field spectra of the non-heme Fe^{2+} active site in metapyrocatechase. Optical absorption (top), CD (middle), and low-temperature MCD (bottom) spectra for metapyrocatechase. ABS and CD spectra were carried out at room temperature. Low-temperature MCD spectrum was recorded at 4.2 K and 5.9 T.

studied exhibited <5% depolarization at 4.2 K.

The effects of azide binding were investigated by the anaerobic addition of microliter quantities of a thoroughly degassed 0.5 M NaN_3/50 mM potassium phosphate buffer (pH 7.5) to deoxygenated metapyrocatechase in the MCD cell. The concentration of azide added to the metapyrocatechase sample in the MCD cell was varied. Up to a 500-fold molar excess of azide relative to the protein (1 mM metapyrocatechase) was used.

Samples of the anaerobic enzyme–substrate complex were prepared by the addition of microliter quantities of a stock solution of 64 mM catechol in 50% glycerol/buffer to metapyrocatechase in the MCD cell. A 10-fold molar excess of substrate over enzyme (1 mM metapyrocatechase) was typically used in the MCD experiments (K_M = 0.015 mM[4b]). Absorption spectra were recorded immediately prior to and following MCD study. Samples used in the MCD work exhibited <2% substrate turnover based on the measured product absorbance at 375 nm (ϵ_{375} = 4.4×10^4 M^{-1} cm^{-1}).[6k] Following low-temperature MCD experiments, samples were thawed to room temperature and the UV/vis spectrum was rerecorded.

Anaerobic ternary azide–enzyme–substrate complex was prepared by the addition of microliter quantities of a stock solution of 5 M NaN_3 in 50% glycerol/buffer to give samples with up to a 50-fold molar excess of azide over enzyme (1 mM metapyrocatechase) when added to the enzyme–substrate sample in the MCD cell. Complete conversion of the metapyrocatechase–catechol sample to metapyrocatechase–catechol–N_3^- was demonstrated by sampling the magnetization behavior at several wavelengths across the ligand field band.

Results

A. Resting Metapyrocatechase. Figure 1 shows the room temperature near-IR optical absorption, CD, and low-temperature MCD spectra for metapyrocatechase. The spectra show one broad low-intensity feature centered at ~11 240 cm^{-1}, which can be assigned as an Fe^{2+} ligand field transition. The position and shape of this band are not affected by the addition of the glassing agent glycerol at room temperature. When cooled to 4.2 K, the peak position and band shape remain approximately the same (Figure 1). Figure 2 shows the room temperature near-IR CD spectrum (650–2150 nm) of metapyrocatechase. This spectrum shows two broad, low-intensity features. The sign and therefore the rotational strength of the CD of the low-energy d → d feature are opposite those of the 11 240 cm^{-1} ligand field band. Due to the interference of solvent overtones in this region, the low-energy band is noisy. On the basis of Gaussian spectral simulations, the low-energy band

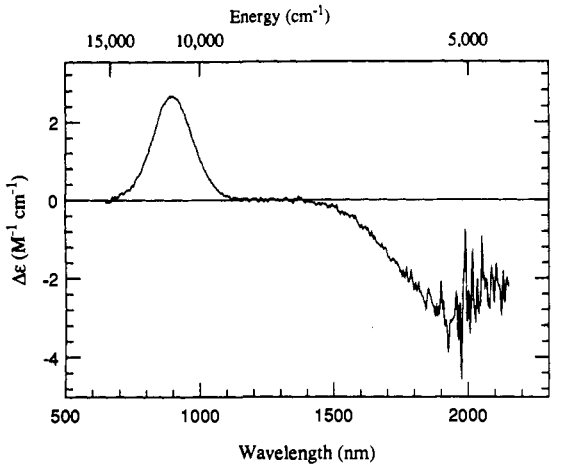

Figure 2. Room temperature near-IR CD spectrum of non-heme Fe^{2+} active site in resting metapyrocatechase.

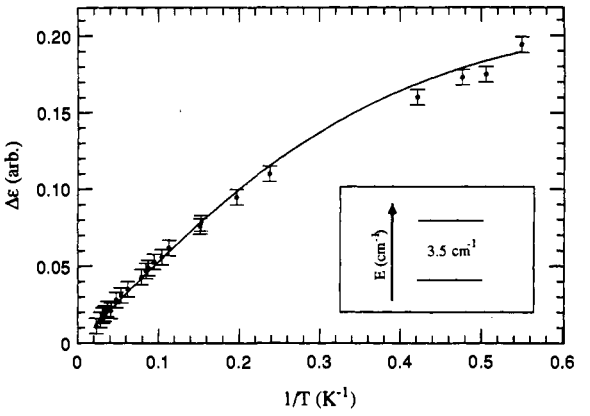

Figure 3. Temperature dependence of metapyrocatechase MCD. Intensity at 0.5 T (●) and fit (—) for metapyrocatechase at 890 nm. Fit obtained for population of two levels is separated by 3.5 cm^{-1}.

appears to be centered at 5220 cm^{-1}.

Figure 3 presents the MCD intensity of the 11 240 cm^{-1} (890 nm) band at 0.5 T as a function of temperature. The MCD intensity is found to increase as the temperature is lowered. This behavior is characteristic of an MCD C-term.[10] C-terms arise due to transitions from a degenerate electronic ground state that splits in a magnetic field. Thus, the large MCD signal at low temperatures indicates that an MCD active doublet sublevel for $S = 2$ is lowest in energy, i.e., $M_s = \pm 2$ must be lowest; hence, $D < 0$. The temperature dependence of the MCD intensity data shows deviations from linear Curie law behavior, which suggests that significant thermal population of low-lying excited states occurs at low temperatures.

The magnetization saturation behavior for metapyrocatechase is presented in Figure 4. MCD intensity curves at constant temperature do not superimpose when plotted as a function of the reduced energy parameter $\beta H/2kT$; i.e., the magnetization curves are nested (Figure 4, left). Nesting of magnetization saturation curves is characteristic of metal sites with $S > {}^1/_2$.[11] The magnetization data also show that the MCD intensity saturates with increasing applied field. When magnetization data are replotted[8] as a function of $1/T$ (Figure 4, right) for fixed field, at lowest temperature, the MCD intensity increases with increasing field, eventually reaching a limiting MCD intensity at high external fields. We have observed similar magnetization saturation be-

(10) (a) Schatz, P. N.; McCaffery, A. J. *Q. Rev., Chem. Soc.* **1966**, *23*, 552. (b) Piepho, S. B.; Schatz, P. N. *Group Theory in Spectroscopy*; Wiley: New York, 1983.

(11) (a) Thompson, A. J.; Johnson, M. K. *Biochem. J.* **1980**, *191*, 411. (b) Johnson, M. K.; Robinson, A. E.; Thomson, A. J. In *Iron Sulfur Proteins*; Spiro, T. G., Ed.; Wiley: New York, 1979; pp 367–406. (c) Werth, M. T.; Johnson, M. K. *Biochemistry* **1989**, *28*, 3982.

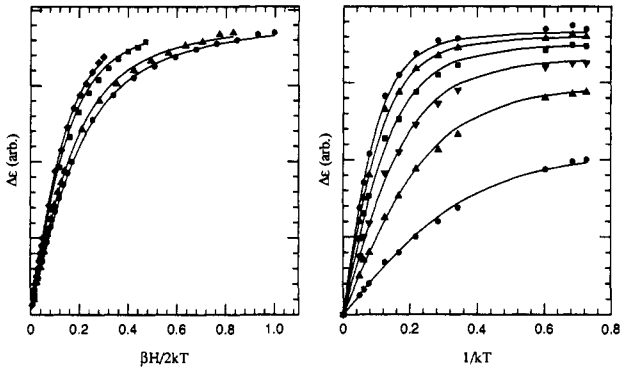

Figure 4. Magnetization saturation behavior for resting metapyrocatechase: (left) MCD amplitude at 890 nm for a range of applied magnetic field strengths (0–5.9 T) at (●) 1.98 K, (▲) 4.2 K, (■), 6.6 K, and (◆) 11.4 K; (right) replot of saturation data shown at left as a function of temperature at constant field for (●) 1.0 T, (▲) 2.0 T, (▼) 3.0 T, (■) 4.0 T, (▲) 5.0 T, and (●) 5.9 T to show field dependence of magnetization saturation behavior at low-temperature limit. Solid curves represent the fit to the data for an isolated non-Kramers doublet with rhombic zero-field splitting. Error bars for individual points are smaller than the symbol size used.

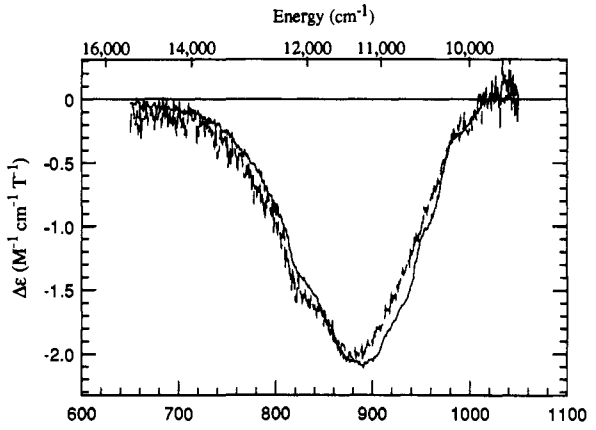

Figure 5. Addition of azide to resting metapyrocatechase: MCD for metapyrocatechase in the absence (—) and presence (---) of 50-fold molar excess of N_3^- at 4.2 K and 5.0 T. All samples were 4 mM in Fe^{2+}.

havior for other ferrous non-heme enzymes and have found that this behavior can be quantitatively explained by a rhombic splitting (δ) of the lowest $M = \pm 2$ ground-state non-Kramers doublet (vide infra). It is important to state that the magnetization data for metapyrocatechase and for each enzyme system described herein has been acquired and analyzed at several different wavelengths within the high-energy ligand field excited-state absorption band. No significant difference in nesting as reflected in the calculated ground-state parameters was observed. Therefore, we conclude that there is no spectroscopic evidence for either the presence of multiple species or the presence of more than one transition within the absorption envelope for any of the metapyrocatechase systems studied.

B. Azide Binding. Figure 5 presents the spectral effects associated with the addition of N_3^- to metapyrocatechase. The ligand field spectrum of the enzyme remains unchanged upon the anaerobic addition of up to a 500-fold molar excess of N_3^- over enzyme. We estimate that an association constant for azide binding of less than 50 M^{-1} could have been measured. There is also no apparent change in the magnetization saturation behavior of the enzyme. Previous study of a series of high-spin Fe(II) square-pyramidal complexes $\{[Fe(TMC)X](BF_4)_2$; TMC = 1,4,8,11-tetramethyl-1,4,8,11-tetraazacyclotetradecane; X = $NCCH_3$, Br, $N_3^-\}$ has shown that changing the axial ligand from N_3^- to Br^- shifts the ligand field excited-state feature by 500 cm^{-1} to lower energy and causes the MCD signal at 4.2 K to saturate much more slowly. Therefore, azide does not appear to bind to the active site of native metapyrocatechase.

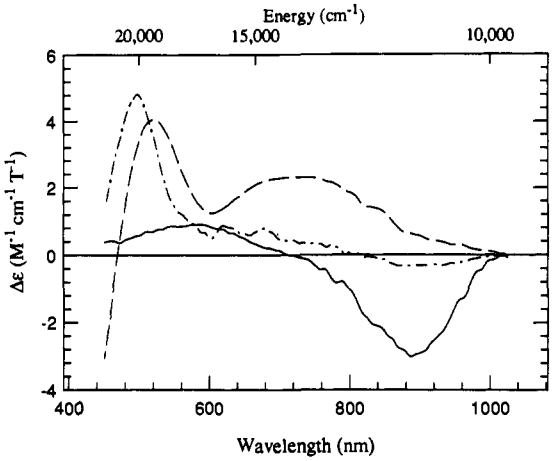

Figure 6. Substrate interactions with metapyrocatechase: MCD spectra of 4.2 K and 5.9 T for native metapyrocatechase (—), metapyrocatechase with anaerobic substrate (– –), and metapyrocatechase with substrate exposed to oxygen (- -).

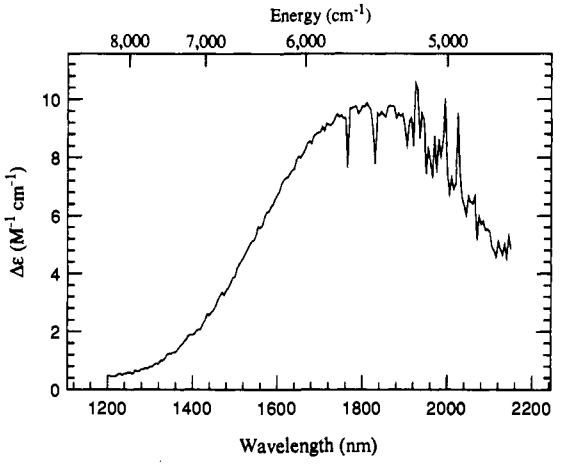

Figure 7. Near-IR CD spectrum of the anaerobic metapyrocatechase–catechol complex at room temperature.

C. Substrate Binding. Dramatic changes occur in the MCD spectrum upon the anaerobic addition of substrate (catechol) to resting metapyrocatechase (Figures 6 and 7). In Figure 6, the low-intensity of d → d excited-state feature in the MCD exhibits the opposite sign and occurs at significantly higher energy (~ 13 330 cm^{-1}) than in uncomplexed metapyrocatechase (ΔE = 2090 cm^{-1}). This new band disappears upon exposure of the sample to O_2 (resulting in conversion of the catechol to product), demonstrating that this band is associated with the Fe^{2+} metapyrocatechase–catechol complex. In addition, upon anaerobic substrate binding, the low-energy d → d excited-state feature in uncomplexed metapyrocatechase is replaced by a band at somewhat higher energy (ΔE = 360 cm^{-1}) with opposite sign in the CD spectrum (Figure 7).

The temperature-dependent MCD data for the metapyrocatechase–catechol complex are shown in Figure 8. The data show increasing MCD signal intensity with decreasing temperature, again indicating a C-term associated with a doublet lowest in energy in the ferrous ground state. These data also exhibit deviations from linear Curie law behavior, indicating thermal population of excited states. However, these deviations from linearity are clearly smaller than those exhibited by uncomplexed metapyrocatechase (cf. Figure 3). The magnetization saturation behavior for the metapyrocatechase–catechol complex is somewhat different from that observed for uncomplexed metapyrocatechase (Figure 9). Magnetization curves obtained for metapyrocatechase–catechol are nested as in resting metapyrocatechase. However, the MCD signal for the metapyrocatechase–catechol complex saturates more quickly, that is, at lower fields for the same temperature than in the native enzyme.

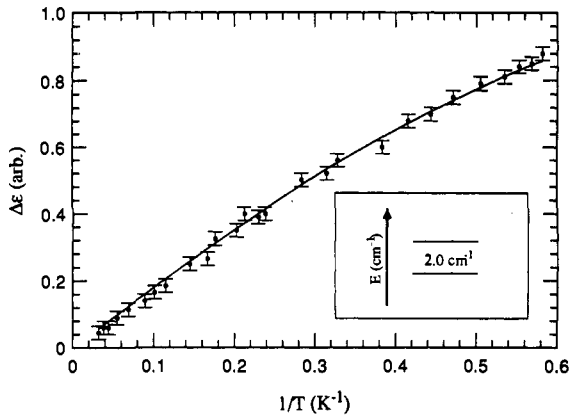

Figure 8. Temperature dependence of metapyrocatechase–catechol MCD: intensity at 0.5 T (●) and fit (—) for anaerobic metapyrocatechase–catechol complex at 750 nm. Fit obtained for the population of two levels is separated by 2.0 cm^{-1}.

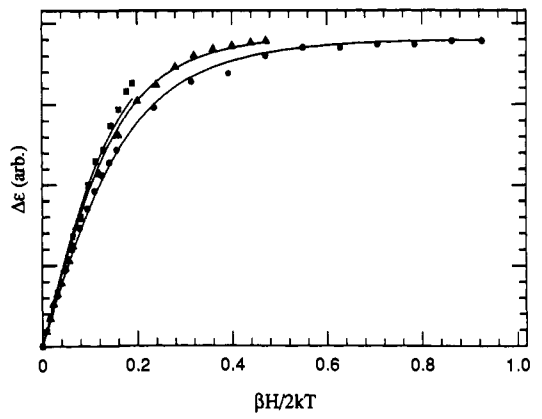

Figure 9. Magnetization saturation behavior of the anaerobic metapyrocatechase–catechol complex: MCD amplitude at 750 nm for a range of applied magnetic field strengths (0–5.9 T) at (●) 2.1 K, (▲) 4.2 K, and (■) 10.5 K. Solid curves represent the fit to the data for an isolated non-Kramers doublet with rhombic zero-field splitting. Error bars for individual points are smaller than the symbol size used.

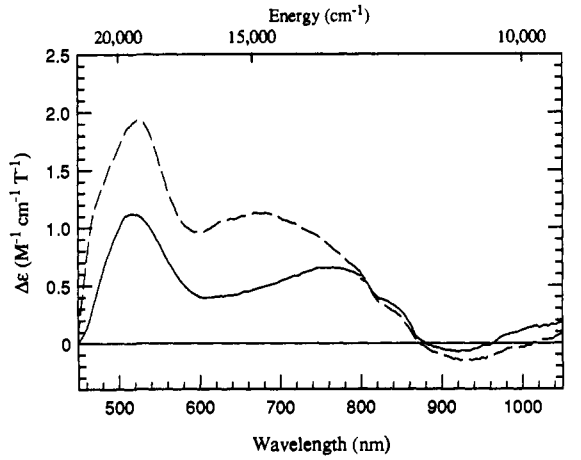

Figure 10. Azide binding to the metapyrocatechase–catechol complex: MCD spectra at 4.2 K and 5.9 T for metapyrocatechase with anaerobic substrate (—), and metapyrocatechase with anaerobic substrate and azide (– –). All samples were 4 mM in Fe^{2+}.

D. Azide Binding to the Enzyme–Substrate Complex. Figures 10 and 11 present the spectral changes associated with the anaerobic addition of a 50-fold molar excess of N_3^- over enzyme (1 mM metapyrocatechase) to the enzyme–substrate complex. Substrate binding thus enhances azide binding by more than 3 orders of magnitude. The d → d excited-state feature centered at 13330 cm^{-1} in the low-temperature MCD spectrum of the enzyme–substrate complex (Figure 10) moves to higher energy

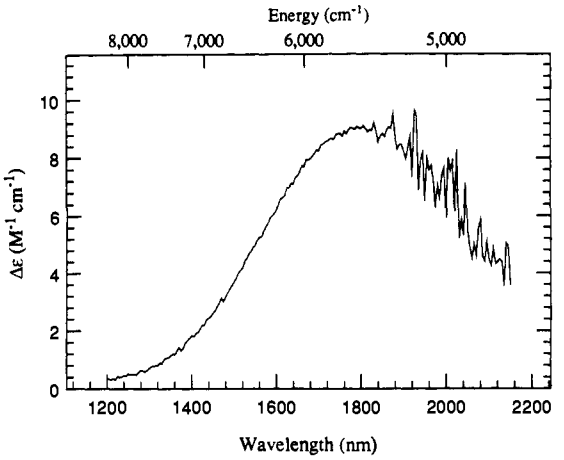

Figure 11. Room temperature near-IR CD spectrum of the metapyrocatechase–catechol–azide complex.

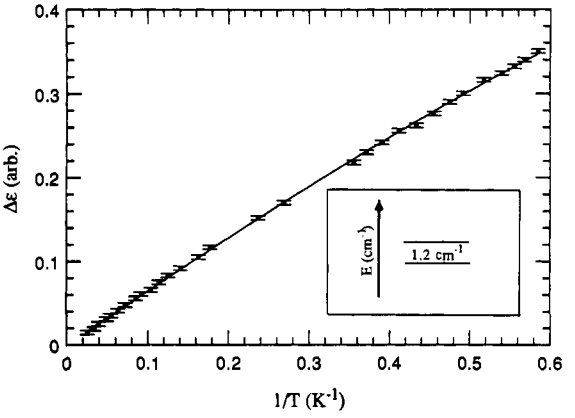

Figure 12. Temperature dependence of metapyrocatechase–catechol–azide complex MCD: intensity at 0.5 T (●) and fit (—) for anaerobic metapyrocatechase–catechol–azide complex at 680 nm. Fit obtained for population of two levels is separated by 1.2 cm^{-1}.

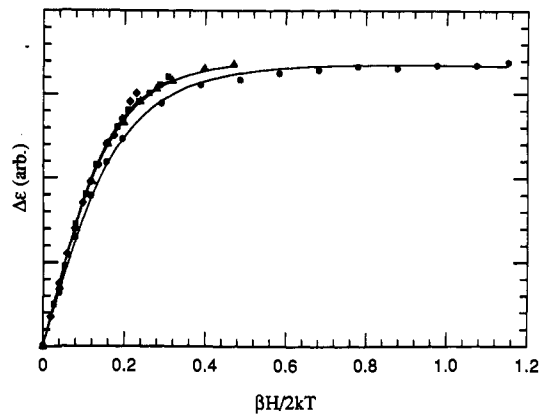

Figure 13. Magnetization saturation behavior of the anaerobic metapyrocatechase–catechol–azide complex. MCD amplitude at 680 nm for a range of applied magnetic field strengths (0–5.9 T) at (●) 1.7 K, (▲) 4.2 K, (■) 6.4 K, and (◆) 8.6 K. Solid curves represent the fit to the data for an isolated non-Kramers doublet with rhombic zfs. Error bars for individual points are smaller than the symbol size used.

by 960 cm^{-1} upon the addition of azide. There is also a small shift in the position of the low-energy d → d band (Figure 11) upon the addition of azide. These spectral changes provide direct evidence that azide binds to the ferrous active site of metapyrocatechase once the metal center is activated by coordination of substrate.

The intensity of the MCD signal centered at 700 nm for the enzyme–substrate–azide complex at fixed field increases with decreasing temperature, indicating that the $M_s = \pm 2$ doublet is lowest in energy in the ground state and that $D < 0$ (Figure 12).

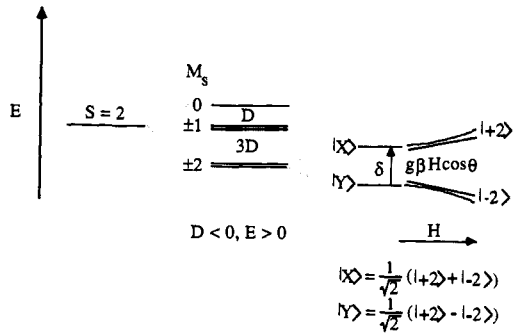

Figure 14. Effect of a magnetic field on a rhombically zero-field-split non-Kramers doublet.

Deviations from linearity in the temperature dependence of the MCD intensity are much smaller than in the enzyme–substrate complex (cf. Figure 8). Magnetization saturation data for the metapyrocatechase–catechol–azide complex again exhibit nesting (Figure 13); however, the MCD signal for metapyrocatechase–catechol–N_3^- saturates much more rapidly than for the metapyrocatechase–catechol complex (cf. Figure 9).

Analysis

A. MCD. The temperature and field dependence of the MCD intensity of the excited-state transitions probe the Fe^{2+} ground state. When the axial zero-field splitting is negative, the MCD active $M_s = \pm 2$ sublevels will be lowest in energy. Thus, the C-term temperature dependence of the MCD intensity indicates that $D < 0$.

The magnetization data for metapyrocatechase form a set of nested curves (Figure 4, left). Replotting the magnetization data for metapyrocatechase as a function of $1/T$ for fixed field (Figure 4, right) reveals that the MCD intensity at low temperature is strongly field-dependent and that the observed field dependence is nonlinear; at high fields at the lowest temperature, the MCD intensity converges to a fixed value. This nonlinear field dependence of the MCD intensity requires a B-term or field-inducing mixing mechanism between sublevels within $g\beta H$ of the lowest sublevel and cannot be simply attributed to thermal population of zero-field-split sublevels.

Previously we showed that field-dependent magnetization saturation behavior similar to that of metapyrocatechase can be modeled by rhombic zero-field splitting within the two sublevels of an isolated non-Kramers $M_s = \pm 2$ doublet (Figure 14).[8] Introduction of a rhombic splitting, of magnitude δ, removes the degeneracy of the non-Kramers doublet sublevels, producing real wave functions, quenching the orbital angular momentum, and eliminating the MCD intensity, which requires complex wave functions. Applying an external magnetic field to the rhombically split non-Kramers doublet changes these wave functions, inducing orbital angular momentum and restoring MCD intensity. The MCD intensity ultimately levels off at the high applied magnetic field limit ($g\beta H > \delta$) where pure complex MCD active levels are produced.

The energy of the two sublevels also changes as the strength of the applied magnetic field is increased. Assuming that the electronic transition involved is purely xy-polarized and that $g_\perp = 0$, the MCD intensity for a rhombically zero-field-split non-Kramers doublet is given by eq 1, where I is the experimental

$$I = A_{\lim\,sat} \int_0^1 \frac{\cos^2\theta}{\left(\frac{\delta^2}{(g_\parallel \beta H)^2} + \cos^2\theta\right)^{1/2}} \tanh\left[\frac{(\delta^2 + (g_\parallel \beta H \cos^2\theta)^2)^{1/2}}{2kT}\right] d\cos\theta \quad (1)$$

MCD intensity, $A_{\lim\,sat}$ is an intensity scaling factor, θ is the angle between the external magnetic field and the molecular zero-field axis, T is the temperature, and k is the Boltzmann constant. Values of $A_{\lim\,sat}$, δ, and $g_\parallel$ are obtained by regressional fitting of experimental magnetization saturation data sets, which consist of the MCD intensity, temperature, and the applied magnetic field strength.

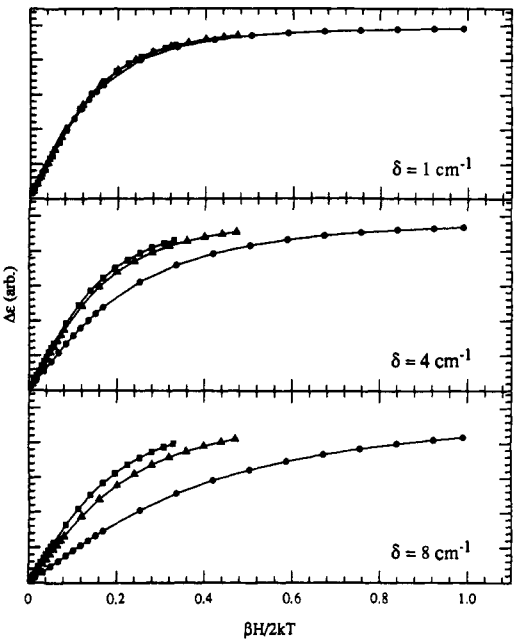

Figure 15. Rhombic zfs effect on the magnetization saturation behavior of an isolated non-Kramers doublet: theoretical saturation data at (●) 2 K, (▲) 4K, and (■) 6 K for (top) $\delta = 1$ cm^{-1}, (middle) $\delta = 4$ cm^{-1}, and (bottom) $\delta = 8$ cm^{-1}.

Figure 15 presents theoretical magnetization saturation plots for an isolated rhombically zero-field-split non-Kramers doublet for varying values of δ. For small values of the rhombic zero-field splitting ($\delta \leq 1$ cm^{-1}), a single magnetization curve is obtained over a wide range of temperatures and applied magnetic fields, consistent with an essentially degenerate doublet lowest in energy. Larger rhombic splitting of the $M_s = \pm 2$ levels (Figure 15b,c) produces the nesting effect. Note that the greater the rhombic splitting, the greater the degree of nesting observed in the magnetization saturation data.

The quality of the calculated fit to the data for uncomplexed metapyrocatechase, metapyrocatechase–catechol, and metapyrocatechase–catechol–azide with use of the isolated non-Kramers rhombic zero-field-split doublet model is excellent (solid lines in Figures 4, 9, and 13).

The validity of the assumptions made in eq 1 have been evaluated in terms of their applicability to the enzyme systems studied here. Specifically, the contribution of a z-polarized transition ($M_z/M_{xy} > 0$) and the effects of a nonzero $g_\perp$ value have been investigated. In this approach, the effective spin Hamiltonian for an isolated non-Kramers doublet has been transformed to the complex basis and augmented with a perpendicular Zeeman term. Since our MCD studies are performed on frozen protein glasses, this Hamiltonian must be incorporated into an expression[12] that takes into account orientation averaging.[11a,12] The integration is accomplished numerically. Parameters M_z/M_{xy} and $g_\perp$ are held constant, while δ, $g_\parallel$, and $A_{\lim\,sat}$ are varied to fit the experimental magnetization saturation data sets. Finally, M_z/M_{xy} and $g_\perp$ are varied to obtain the optimal fit. Solutions have been tested for uniqueness by selecting initial values of all the parameters over a wide range.

Values of δ, $g_\parallel$, $g_\perp$, and M_z/M_{xy} obtained from this general treatment for uncomplexed metapyrocatechase and substrate- and azide-bound metapyrocatechase are summarized in Table I. In general, $g_\perp$ is close to zero, and the values obtained for δ and $g_\parallel$

(12) Schatz, P. N.; Mowery, R. L.; Krausz, E. R. *Mol. Phys.* **1978**, *35*, 1537.

Table I. Experimental Ground-State and Excited-State Splittings and Ligand Field Parameters

active site complex	sign of MCD	$d_{x^2-y^2}$ (cm^{-1})	d_{z^2} (cm^{-1})	ΔE_{Curie} (cm^{-1})	δ (cm^{-1})	$g_\parallel$	$g_\perp$	M_z/M_{xy}	$-\Delta$ (cm^{-1})	V (cm^{-1})
metapyrocatechase	-	11 240	5220	3.5	4.0	8.9	0.25	-1.0	600	300
metapyrocatechase-N_3^-	-	11 240			3.6	8.6	0.25	-1.0	600	300
metapyrocatechase-catechol	+	13 330	5580	2.0	2.6	8.4	0.25	1.0	1100	704
metapyrocatechase-catechol-N_3^-	+	14 290	5610	1.2	1.8	8.3	0.25	1.0	1500	500

are in excellent agreement with those obtained through use of eq 1. The rhombic zero-field splitting was found to vary (metapyrocatechase, δ = 4.0 cm^{-1}; metapyrocatechase-catechol, δ = 2.6 cm^{-1}; metapyrocatechase-catechol-azide, δ = 1.8 cm^{-1}). However, for all complexes studied, $\delta \leq 4.0$ cm^{-1}. Binding substrate and then azide to the uncomplexed enzyme produces a significant decrease in the magnitude of the rhombic zero-field splitting consistent with the reduced nesting observed in Figures 4, 9, and 13, respectively. This trend indicates that significant changes occur in the ferrous ground state and therefore in the ferrous active site structure of these systems.

Since the magnetization saturation data for the metapyrocatechase systems studied are consistent with rhombic zero-field splitting within an isolated $M_s = \pm 2$ doublet, deviations from Curie behavior (nonlinearity) in the temperature dependence of the MCD intensity at small fixed field (Figures 3, 8, and 12) are due to Boltzmann population of the rhombically zero-field-split $M_s = \pm 2$ doublet sublevels and should provide an independent estimate of the degree of rhombic zero-field splitting in the ground state. Since the two sublevels are conjugate states, the contribution of the C-term for each state ($\mathcal{A}$) is equal and opposite in sign. Therefore, for two sublevels split by an energy (E_{Curie}), the temperature dependence of the MCD intensity I for an isolated rhombically split non-Kramers doublet is given by eq 2. The

$$I = \mathcal{A}(1 - e^{-E_{Curie}/kT})/(1 + e^{-E_{Curie}/kT}) \quad (2)$$

MCD data have been fit to eq 2 by regression analysis, leaving $\mathcal{A}$ and E_{Curie} as adjustable parameters. The initial value of $\mathcal{A}$ has been estimated from the MCD data at lowest temperatures, assuming that only the lowest sublevel is populated. The quality of the fits to the MCD data for metapyrocatechase, metapyrocatechase-catechol, and the ternary metapyrocatechase-catechol-azide complex are excellent and are represented by solid lines in Figures 3, 8, and 12, respectively. Values of the rhombic zero-field splitting estimated from the temperature dependence of the MCD data are given in Table I. The energies calculated via the temperature dependence are all small (<4 cm^{-1}) and decrease significantly as substrate and subsequently azide are introduced into the metapyrocatechase active site. This trend in E_{Curie} is consistent with the trend in the δ values, obtained from the temperature- and field-dependent MCD intensity with eq 1. In addition, the absolute magnitudes of δ and E_{Curie} for metapyrocatechase, metapyrocatechase-catechol, and the metapyrocatechase-catechol-azide complex agree to within their respective experimental uncertainties (±0.5 cm^{-1}).

B. Ligand Field. In a cubic ligand field, the ^5D ground state of the free d^6 ion splits into $^5T_{2g}$ and ^5E_g orbital states, with the ^5E_g excited state at $10Dq$ (Figure 16). For biologically relevant ligands (N and O type), the energy splitting between the $^5T_{2g}$ and ^5E_g orbital states is on the order of 10 000 cm^{-1}. Low symmetry distortions of the octahedron produce an additional splitting of the ^5E_g excited state of <2000 cm^{-1}.[13] Removal of one axial ligand produces a 5-coordinate square-pyramidal geometry and an excited-state ^5E splitting of >5000 cm^{-1}. The energy of the highest energy spin-allowed ligand field band is >10 000 cm^{-1} for square-pyramidal coordination.[14] Five-coordinate trigonal-bipyramidal complexes also have two d → d bands, one at <10 000 cm^{-1} and a second near 5000 cm^{-1}.[15,16] Tetrahedral Fe^{2+} exhibits spin-allowed $^5E \rightarrow {}^5T_2$ ligand field transitions at ~5000 cm^{-1} ($10Dq_{tet} = -(4/9)10Dq_{oct}$), while 4-coordinate square-planar ferrous complexes may be distinguished by the presence of an unusually high energy ligand field transition near 20 000 cm^{-1}.[17]

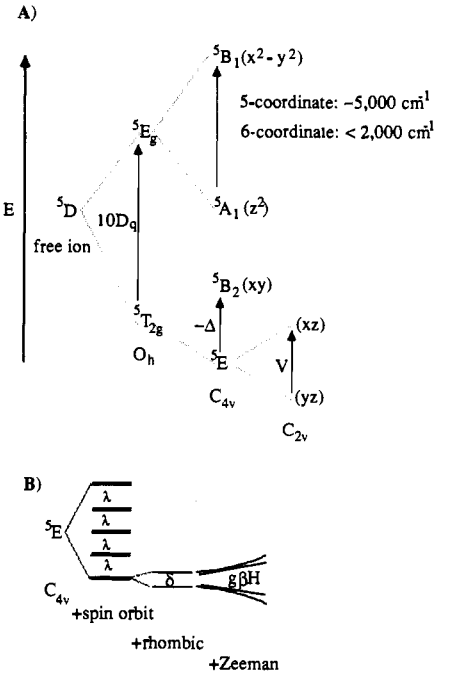

Figure 16. Ground-state splitting pattern for a $^5T_{2g}$ ground state predicted by a ligand field Hamiltonian description: (a) An axial perturbation produces an orbitally degenerate ^5E ground state lowest in energy. (b) In-state spin-orbit coupling results in five doublets split by λ. Note that this pattern differs significantly from that predicted with a pure spin Hamiltonian (Figure 14).

In resting metapyrocatechase, two d → d excited-state features are observed, one at 11 240 cm^{-1} and the second at 5220 cm^{-1} (Figures 1 and 2), which is consistent with a square-pyramidal limiting description for the metapyrocatechase Fe^{2+} active site. Similarly, for the metapyrocatechase-catechol and the ternary metapyrocatechase-catechol-azide complexes, one d → d transition is found at energies >10 000 cm^{-1} and a second near 5000 cm^{-1} (Figures 6, 7, 10, and 11). Thus, 5-coordinate square-pyramidal geometry is the effective site symmetry for the ferrous non-heme active site in these systems as well.

The ^5E splitting increases dramatically upon substrate and small molecule binding. The highest energy $d_{x^2-y^2}$ orbital shows the most variation in energy, between 11 240 and 14 290 cm^{-1}, such that the magnitude of the ^5E excited-state splitting changes from 6020 to 8680 cm^{-1}. Since the ^5E excited-state splitting is sensitive to ligand σ interactions, the variations observed in the ^5E signify that the active site structure has been significantly changed by the addition of catechol and then azide.

(13) (a) Holmes, O. W.; McClure, D. S. *J. Chem. Phys.* **1957**, *26*, 1686. (b) Cotton, F. A.; Meyers, M. D. *J. Am. Chem. Soc.* **1960**, *82*, 5023. (c) Goodgame, D. M. L.; Goodgame, M.; Hitchman, M. A.; Weeks, M. J. *Inorg. Chem.* **1965**, *5*, 635. (d) Loehr, J. S.; Loehr, T. M.; Mauk, A. G.; Gray, H. B. *J. Am. Chem. Soc.* **1980**, *102*, 6992.

(14) (a) Riley, D. P.; Merrell, P. H.; Stone, J. A.; Busch, D. H. *Inorg. Chem.* **1975**, *14*, 490. (b) Hodges, K. D.; Wollman, R. G.; Barefield, E. K.; Hendrickson, D. N. *Inorg. Chem.* **1977**, *16*, 2746.

(15) The ferric site of the intradiol dioxygenase protocatechuate 3,4-dioxygenase has recently been shown to have a trigonal-bipyrimidal geometry: Ohlendorf, D. H.; Lipscomb, J. D.; Weber, P. C. *Nature (London)* **1988**, *336*, 403.

(16) Ciampolini, M.; Nardi, N. *Inorg. Chem.* **1966**, *5*, 1150. (b) Chia, P. S. K.; Livingstone, S. E. *Aust. J. Chem.* **1969**, *22*, 1613. (c) Stoppioni, P.; Mani, F.; Sacconi, L. *Inorg. Chim. Acta* **1974**, *11*, 227.

(17) Burns, R. G.; Clark, M. G.; Stone, A. J. *Inorg. Chem.* **1966**, *5*, 1268.

Lowering the symmetry from octahedral splits the $^5T_{2g}$ orbital state into ^5E and $^5B_2$ components (see Figure 16a). When D is positive, the $^5B_2$ component is lowest, while when D is negative, the ^5E component is lowest in energy.[8] Since a negative value of D is observed for the temperature-dependent MCD of metapyrocatechase, the ^5E component of the $^5T_{2g}$ is lowest. Thus, there is orbital (E) as well as spin degeneracy in the ground state, and the effects of in-state spin–orbit coupling on the ground-state splitting must be included.[8b] The ground-state energy level scheme produced by a more general ligand field Hamiltonian description[8b] is shown in Figure 16b. The ground-state splittings in Figure 16b differ significantly from Figure 14 in that axial orbital splitting plus spin–orbit coupling produces five equally spaced doublets separated by λ, where λ is the Fe^{2+} spin–orbit coupling parameter and is approximately -80 cm^{-1}. Rhombic zero-field splitting of the lowest doublet corresponds to δ.

With use of this ligand field Hamiltonian description, δ and $g_\parallel$ have been calculated for the lowest rhombically split doublet as a function of the degree of ground-state axial (Δ) and rhombic (V) orbital splitting (Figure 16b). The results of these calculations are shown in Figure 13 of ref 8b. Small axial orbital splittings ($-\Delta < 500$ cm^{-1}) result in large rhombic zero-field splittings ($\delta > 6$ cm^{-1}) and characterize an octahedral geometry, while large axial orbital splittings ($-\Delta > 1000$ cm^{-1}) produce small rhombic zero-field splitting ($\delta < 4$ cm^{-1}) and reflect square-pyramidal coordination.

Values of $-\Delta$ and V have been calculated for metapyrocatechase, metapyrocatechase–catechol, and the ternary metapyrocatechase–catechol–azide complex from the experimentally derived δ and $g_\parallel$ values as described in ref 8b and are summarized in Table I. The $^5T_{2g}$ ground-state splitting increases from 750 cm^{-1} for metapyrocatechase to almost 2000 cm^{-1} for the enzyme–substrate–azide complex. Upon substrate binding, both the ground-state axial and rhombic orbital ground-state splitting increase. Addition of azide to the anaerobic enzyme–substrate complex further increases the axial orbital splitting while decreasing the ground-state rhombic splitting. Since the ground state $^5T_{2g}$ splittings are sensitive to ligand π interactions, these variations show that significant changes in the active site ligand bonding occur in the presence of catechol and azide.

Discussion

Since the Fe^{2+} ligand field transitions provide the energies of the $d_{x^2-y^2}$ and d_{z^2} orbitals relative to the ground state and since values of $-\Delta$ and V obtained from the ground-state analysis give direct information on the relative energies and ordering of the d_{xy}, d_{xz}, and d_{yz} orbitals (Figure 16), we can now construct an experimentally derived ligand field energy level diagram for the Fe^{2+} active site in each of the metapyrocatechase systems studied (Figure 17). These experimental energy level diagrams provide insight into the geometry and electronic structure of the metapyrocatechase active site and into structural changes in the active site due to substrate and azide binding of relevance to catalysis.

Both the excited-state and ground-state spectroscopic data and the resulting ligand field energy level diagram reflect a 5-coordinate square-pyramidal geometry as the most accurate limiting description for the Fe^{2+} active site in the resting as well as the substrate- and azide-bound forms of metapyrocatechase. However, there is clearly significant variation in ligand field energy level splittings over these forms of the metapyrocatechase active site. Addition of substrate dramatically perturbs the d orbital splitting, indicating that a substantial change has taken place in the geometric and electronic structure of the Fe^{2+} active site. These large changes suggest substrate directly interacts with the Fe^{2+} center and likely binds to it. The $d_{x^2-y^2}$, d_{xy}, and d_{xz} orbitals in the metapyrocatechase–catechol complex are significantly destabilized relative to the orbital energy levels in the uncomplexed enzyme (Figure 17, leftmost and center diagrams). The marked destabilization of the $d_{x^2-y^2}$ and d_{xy} orbitals is consistent with the Fe^{2+} center moving into the equatorial ligand plane. Since catechol is a poor ligand for Fe^{2+}, this strongly supports an axial coordination mode for this ligand. The destabilization of d_{xz} indicates

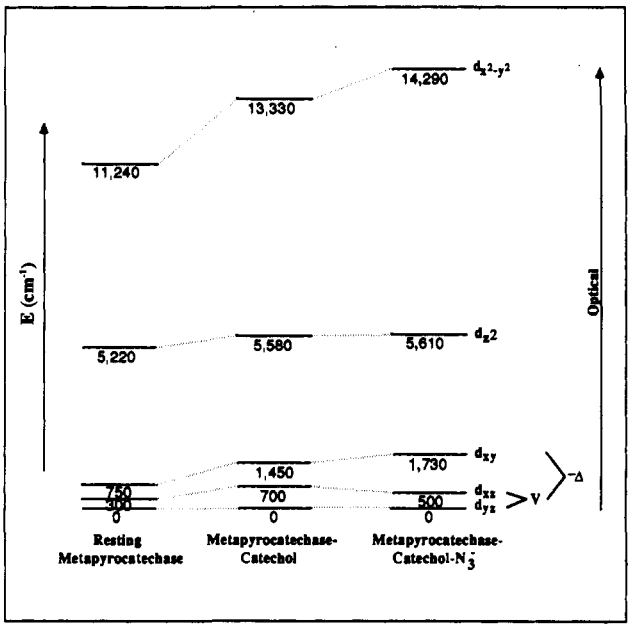

Figure 17. Experimentally derived ligand field energy level diagram for uncomplexed metapyrocatechase (left), metapyrocatechase–catechol (center), and metapyrocatechase–catechol–azide (right) constructed with use of the information summarized in Table I. Note that the energy of each orbital level is referenced to the ground state (d_{yz}), which is defined as 0 cm^{-1}. The splitting $-\Delta$ is the difference of the d_{xy} orbital energy and the average energy of the d_{xz} and d_{yz} orbitals.

that a significant change also occurs in equatorial bonding. Therefore, catechol appears to bind as a bidentate ligand and occupies the axial and one equatorial ligation position in the 5-coordinate square-pyramidal active site of the enzyme–substrate complex. Evidence for the possibility of bidentate coordination of catechol analogues to the metapyrocatechase active site iron also comes from the observation of superhyperfine coupling in the EPR spectra of the enzyme–nitrosyl adduct complexed with protocatechuate specifically labeled with ^{17}O ($I = {}^5/_2$) at either the 3- or 4-hydroxyl position.[4c]

Significant changes in the ligand field energy levels also occur with azide binding to the Fe^{2+} center of the anaerobic enzyme–substrate complex. The destabilization of the $d_{x^2-y^2}$ and d_{xy} orbitals is consistent with further lowering of the Fe^{2+} into the equatorial ligand plane. In addition, the d_{xz} orbital is somewhat stabilized compared to that of the enzyme–substrate complex. These spectral changes are consistent with coordination of a relatively strong field azide to the ferrous center in the equatorial plane.

Previously, an ordered bi–uni mechanism where E is enzyme, S is substrate (catechol), and P is product (α-hydroxymuconic ϵ-semialdehyde) had been proposed for metapyrocatechase catalysis.[6g] Accordingly, no evidence for reaction of the enzyme

$$E + S \rightarrow E\text{-}S$$

$$E\text{-}S + O_2 \rightarrow E\text{-}S\text{-}O_2$$

$$E\text{-}S\text{-}O_2 \rightarrow E + P$$

with O_2 or formation of an $E\text{-}O_2$ complex in the absence of substrate has been reported. The mechanism by which this ordering is effected remains obscure although we have proposed from previous studies that it is due to energetic coupling of the substrate and O_2-binding reactions.[4b] The spectroscopic information derived here provides a method to directly investigate the structure of the resting enzyme and its substrate complex. Moreover, to the extent that N_3^- binding models O_2 binding, information about the ternary enzyme complex can be derived. The structural information obtained from the present study of the active site of metapyrocatechase is summarized in Figure 18. The active site of the enzyme as isolated binds substrate effectively yet is unable to bind azide. This is interesting in that azide is a better ligand than catechol for Fe^{2+} in model compounds. Upon substrate

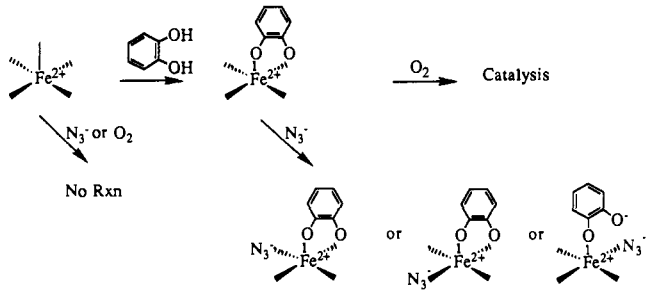

Figure 18. Spectroscopically effective structural mechanism for the Fe^{2+} active site in metapyrocatechase.

binding, however, azide readily coordinates to the active site iron.[18] Thus, substrate binding activates the iron active site of metapyrocatechase toward small molecule binding. Similar activation toward O_2 binding would account for the observed ordered kinetic mechanism. Moreover, formation of a complex with both substrate and O_2 bound to an Fe^{2+} center prior to catalysis would be consistent with the current mechanistic proposal for the enzyme.[4c] The formation of such a complex is thought to be a primary distinguishing characteristic between the mechanisms of extra- and intradiol dioxygenases;[4b,c] in the case of the latter enzymes, O_2 is proposed to react with the substrate active iron chelate by direct attack on the substrate rather than the iron.[19]

One possible explanation for the substrate-activated binding of azide in metapyrocatechase is that substrate binding induces a conformational change in the protein near the active site. Since azide does not bind to the iron in the absence of catechol, yet catechol, the poorer ligand in model complexes, does bind, interaction of substrate with the protein pocket appears to play an important role in binding catechol to the ferrous center. The change in sign of the 5220 cm^{-1} d → d band of metapyrocatechase (cf. Figures 2 and 7) and the previously observed appearance of a new UV CD feature at 317 nm[6f] are consistent with a local protein conformational change occurring with substrate binding to the Fe^{2+} active site. This substrate-induced protein conformational change would activate an exchangeable coordination position at the ferrous center for exogenous ligand binding.

Activation of the ferrous center toward exogenous ligand binding may also result from electronic effects. Upon substrate binding, the Fe^{2+} center moves into the equatorial ligand plane. This improves the potential for σ orbital overlap with small molecules such as azide (or potentially molecular oxygen), which we have determined to bind to an equatorial ligand site. From Figure 17, catechol binding strongly splits the $^5T_{2g}$ ground state, localizing the extra electron in the d_{yz} orbital,[20] along one equatorial bond axis. This localized anisotropic electron density should weaken the bonding interaction with a donor ligand in the equatorial plane while activating the Fe^{2+} center toward reaction at this position with electron-acceptor ligands, in particular O_2. From ligand field arguments (catechol being a weak field ligand), one might expect this electron density in the d_{yz} orbital to the localized along and trans to the equatorial catechol binding axis. However, a space-filling model indicates that the cis position is structurally more reasonable for oxygen attack of substrate at the 3-position. Therefore, these possibilities are included in Figure 18. A third possibility for the ternary metapyrocatechase–catechol–azide complex, included in Figure 18, is also consistent with our data. In this model, azide replaces the equatorial catechol coordination site in the enzyme–substrate complex. Thus, catechol would then coordinate in a monodentate fashion to the Fe^{2+} center in the ternary complex. In this model, the ferrous center would be bound to three rather than two protein-based donor ligands.

Recently, the EPR spectra of nitric oxide complexes of non-heme Fe^{2+} metalloenzymes including metapyrocatechase has been used as a spectroscopic probe of ferrous active site structure.[4b,c] These NO complexes have an electronic spin of $S = {}^3/_2$ and exhibit distinctive intense EPR signals with g values near 2 and 4 consistent with a very close to axial electronic structure ($E/D < 0.03$). The structural information concerning the active site of metapyrocatechase and its ligand complexes gained from these studies compliments that of the current study in many aspects. Specifically, substrate appears to form a bidentate complex with the iron in the nitrosyl complex. In doing so, the electronic environment of the iron is substantially altered. The principle difference between N_3^- and NO binding appears to be that NO can bind to the Fe^{2+} even in the absence of substrate. However, the binding affinity of NO is increased by 2 orders of magnitude by substrate binding[4b] reminiscent of the interconnection of substrate and N_3^- binding demonstrated here.

In summary, these studies have demonstrated the sensitivity of this spectroscopic protocol in probing Fe^{2+} active site structural changes associated with ligand binding. We have found that substrate coordinates to the 5-coordinate square-pyramidal ferrous active site of metapyrocatechase, that substrate binding activates metapyrocatechase toward small molecule binding (and O_2 reactivity), and that azide binds to the ferrous active site. Furthermore, azide inhibits turnover of metapyrocatechase. Therefore, the metapyrocatechase–catechol–azide complex may be an important stable small molecule analogue of the mechanistically significant ternary metapyrocatechase–catechol–dioxygen complex. The ternary azide complex has a 5-coordinate square-pyramidal structure with azide bound in the equatorial ligand plane. Significant insight into the origin of this substrate-induced activation of small molecule reactivity is derived from the electronic structure of this site obtained from the MCD-derived ligand field splitting of the d orbitals. We are at present extending this spectroscopic protocol to probe substrate and small molecule interactions in a number of other mononuclear non-heme high-spin Fe^{2+} enzyme systems.

Acknowledgment. This research was supported by the National Institute of Health (Grant GM40392 (E.I.S.) and GM24689 (J.D.L.)). P.A.M. thanks the N.I.H. for a postdoctoral fellowship (Grant GM12333). We also acknowledge the acquisition of preliminary spectroscopic data on uncomplexed metapyrocatechase by Dr. James W. Whittaker.

Registry No. Fe, 7439-89-6; N_3, 14343-69-2; HO-*o*-C_6H_4-OH, 120-80-9; metapyrocatechase, 9029-46-3; dioxygenase, 37292-90-3.

(18) N_3^- acts as an inhibitor of the enzyme turnover consistent with its observed interaction with the active site iron. However, the inhibition is uncompetitive with respect to catechol, and no inhibition is observed with respect to O_2. Thus, the mechanism of inhibition is complex.

(19) (a) Que, L., Jr.; Lipscomb, J. D.; Münck, E.; Wood, J. M. *Biochem. Biophys. Acta* **1977**, *485*, 60. (b) Whittaker, J. W.; Lipscomb, J. D. *J. Biol. Chem.* **1984**, *259*, 4487.

(20) The rhombic splitting parameter V in Figure 16 is defined so as to produce a d_{yz} orbital ground state, which however is oriented by the ligand field at the Fe^{2+} site.